involve
a journal of mathematics

Hitting time of Brownian motion subject to shear flow

Despina Chouliara, Yishu Gong, Siming He, Alexander Kiselev, James Lim, Omar Melikechi and Keenan Powers

msp

2022 vol. 15, no. 1

INVOLVE 15:1 (2022)
https://doi.org/10.2140/involve.2022.15.131

Hitting time of Brownian motion subject to shear flow

Despina Chouliara, Yishu Gong, Siming He, Alexander Kiselev, James Lim, Omar Melikechi and Keenan Powers

(Communicated by Suzanne Lenhart)

The 2-dimensional motion of a particle subject to Brownian motion and ambient shear flow transportation is considered. Numerical experiments are carried out to explore the relation between the shear strength, box size, and the particle's expected first hitting time of a given target. The simulation is motivated by biological settings such as reproduction processes and the workings of the immune system. As the shear strength grows, the expected first hitting time converges to the expected first hitting time of the 1-dimensional Brownian motion. The dependence of the hitting time on the shearing rate is monotone, and only the form of the shear flow close to the target appears to play a role. Numerical experiments also show that the expected hitting time drops significantly even for quite small values of shear rate near the target.

1. Introduction

We consider the following stochastic differential equation (SDE) subject to the initial condition $X_{t=0} = x_0$ on the torus $\mathbb{T}^2 = [0, L)^2$:

$$\begin{pmatrix} d(X_1)_t \\ d(X_2)_t \end{pmatrix} = \begin{pmatrix} Au((X_2)_t) \\ 0 \end{pmatrix} dt + \sqrt{\nu} \begin{pmatrix} d(B_1)_t \\ d(B_2)_t \end{pmatrix}, \tag{1-1}$$

where $B_{1,2}$ are independent standard Brownian motions. This SDE models a single diffusing agent advected by shear flow. The vector $X_t = ((X_1)_t, (X_2)_t)$ denotes the position of the agent. The ambient fluid stream is assumed to be shear flow $(Au((X_2)_t), 0)$ with the amplitude coupling constant A. We are interested in the expected hitting time of a target located at the center of the torus $\left(\frac{L}{2}, \frac{L}{2}\right)$ when the random swimmer starts at $(0, 0)$. Our motivation for this study originates in biology, in particular reproduction processes where sperm are searching for eggs, immune system workings where killer T-cells are looking for invading bacteria or viruses,

MSC2020: 35K10, 60G07, 92B05.
Keywords: hitting time, shear flow.

or pollinators foraging for nectar. One can also envision a microrobot seeking some target. In all these situations, the search happens in the ambient fluid, and often the relevant spatial scales are such that the fluid flow can be regarded as shear. In many of the described settings, there is another factor present — chemotaxis. For example, eggs secrete pheromones that are attractive for sperm. The chemotaxis effect will not be part of our analysis here and will be addressed elsewhere. Our analysis is set in two dimensions due to computing power limitations, but also because some of the relevant processes take place effectively in two dimensions (like, for example, reproduction for marine animals which happens on the surface of the ocean).

This work has been especially influenced by the detailed experiment by Riffell and Zimmer on fertilization success rates of marine species such as abalone and its dependence on the ambient flow shear rates and presence vs. absence of chemotaxis. Marine animals such as abalones, corals, and shrimp release their eggs and sperm into the fluid stream. The gametes are positively buoyant and rise to the surface of the ocean. The eggs are not mobile but release attractive chemicals. Simultaneously, the sperm aggregate towards the eggs by a combination of random Brownian motion, ambient flow, and chemotaxis-aided directed transport. In [Riffell et al. 2004; Riffell and Zimmer 2007; 2011] the researchers put well-mixed abalone sperm and eggs into a Taylor–Couette tank. They observed that the effect of shear flow is two-fold. If the shear flow speed is moderately slow, the shear enhanced fertilization success rates. On the other hand, if the shear flow speed is faster than a certain threshold, the shear overwhelms the gametes' motility. It looks likely that even though the sperm approach the eggs, they cannot stay close and attach to them, and the failure in attachment results in a dropping fertilization rate. The sperm are evenly distributed in the seawater in the biological experiment, and the experimental time is quite limited (≈ 15 seconds). The eggs are introduced into the mixture through specific openings in the tank. Hence only the *group of sperm* surrounding the eggs have access to the egg zone. As a result, the *microflow* environment described by shear flow plays a dominant role during the fertilization process under this setup.

In this paper, we explore the fluid-fertilization interaction from a different point of view, an idealized situation where there is just a single agent searching a single target. Thus in the context of the fertilization process, we focus on the searching success of an *individual sperm*, whose initial position may be *distant* from the egg. To quantify the success of the fertilization, we consider the first hitting time of the target, i.e.,

$$T_{x_0}(\omega) = \min\{\tau \mid X_\tau(\omega) \in E_\delta\}. \tag{1-2}$$

Here $X_\tau(\omega)$ is the realization of the solution to the stochastic differential equation (1-1). In particular, we are interested in the dependence of the hitting time on the parameters of the problem such as A and L. Notice that two of the parameters — such as for example ν and the size of the target — can be normalized by rescaling

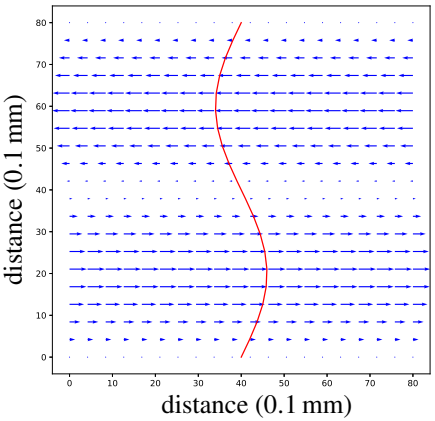

Figure 1. Shear strength multiplied by $dt = 0.01s$.

space and time. Our study is primarily numerical: we implement a numerical scheme to characterize the relative importance of each factor.

The first hitting/exit time of the Brownian motion is a traditional topic in stochastic analysis. It is closely related to the study of elliptic equations on bounded domains, as we will recall below. We also refer to the classical books, e.g., [Durrett 1996; Øksendal 1989]. In the case of the fast ambient shear flow $A(u(x_2), 0)$, see Figure 1, one expects that as the shear rate A approaches infinity, it serves as a dimension-reduction mechanism. Namely, the 2-dimensional SDE dynamics get homogenized in the shear direction, and the effective dynamics become 1-dimensional Brownian motions. This expectation is rigorously confirmed in a variety of settings by Freidlin–Wentzell theory [2012]. In the case of the general ambient stream u, the vector fields' influence on the first exit time on a bounded domain in $\mathbb{R}^2$ was explored in [Iyer et al. 2010]. Our experiments confirm the dimension-reduction phenomena and provide a detailed picture of the transition from fully 2-dimensional hitting time to 1-dimensional as the amplitude A increases (with fixed box size L). In particular, the dependence of the hitting time on A is monotone decreasing. One aspect that we found surprising is the significant reduction in expected hitting time already at quite low values of the shear rate. We also experimented with varying the shear profile away from the horizontal strip containing the target and noted that the expected hitting time did not change as a result.

We focus on the following geometric configuration in our numerical exploration. The domain $\mathbb{T}^2$ has dimension $[0, L)^2$. The target is stationary and is described by a disk $E_\delta = B\left(\left(\frac{L}{2}, \frac{L}{2}\right); \delta\right)$. In all our simulation we will have $L \gg \delta$. The shear profile is adapted to the size of the torus

$$u(x_2) = \sin\left(\frac{2\pi\left(x_2 - \frac{L}{2}\right)}{L}\right)$$

and to the location of the target at $x_2 = \frac{L}{2}$ — we can think of the fluid flow as measured relative with respect to the target. The agent starts its search at the point $(0, 0)$, which is distance $\sim \frac{L}{2}$ away from the target in both directions. In the numerical experiment, we ran multiple simulations and calculated the average hitting time. The Euler–Maruyama method (see, e.g., [Kloeden and Pearson 1977]) is applied to simulate the motion of the agent.

2. Mathematical analysis

2.1. ***Expected first hitting times.*** In this section, we consider some analytic estimates of the expected time for the particle to hit the egg. We begin with the computation of one-dimensional hitting time that will serve as the limit of the 2-dimensional hitting time as $A \to \infty$. In the 1-dimensional analog of our problem, the agent starts at $x_0 = 0$ and performs a Brownian motion $\sqrt{\nu} dB_t$ on $[0, L)$ with periodic boundary conditions until it hits the interval $\left[\frac{L}{2} - \delta, -\frac{L}{2} + \delta\right]$. We can recast this problem equivalently as the exit time from $\left[-\frac{L}{2} + \delta, \frac{L}{2} - \delta\right]$ for a Brownian particle starting at 0. The expectation of such an exit time is well known and can be computed explicitly; we provide a brief sketch of the argument. First recall the Dynkin formula [Øksendal 1989]: For $f \in C_0^2$, suppose τ is a stopping time, $\mathbb{E}^x[\tau] < \infty$. Then

$$\mathbb{E}^x[f(X_\tau)] = f(x) + \mathbb{E}^x\left[\int_0^\tau Hf(X_s)\, ds\right], \tag{2-1}$$

where in our case

$$dX_t = \sqrt{\nu} dB_t, \quad Hf = \tfrac{1}{2}\nu \partial_{xx} f. \tag{2-2}$$

To apply the formula, we consider the solution f to the partial differential equation

$$\tfrac{1}{2}\nu \partial_{xx} f = -1, \quad f\left(\pm\tfrac{L}{2} \mp \delta\right) = 0. \tag{2-3}$$

Combining the equation and the formula (2-1), we obtain the relation

$$0 = f(X_\tau) = f(x) + \mathbb{E}^x\left[\int_0^\tau Hf(X_s)\, ds\right] = f(x) - \mathbb{E}^x[\tau], \tag{2-4}$$

which in turn yields that

$$f(x) = \mathbb{E}^x[\tau]. \tag{2-5}$$

Directly solving the equation yields that

$$f(x_0) = -\frac{1}{\nu} x_0^2 + \frac{1}{\nu}\left(\frac{L}{2} - \delta\right)^2. \tag{2-6}$$

By plugging $x_0 = 0$ in the formula (2-6), we obtain that the average first hitting time is

$$\mathbb{E}^{x_0}[T_{1D}] = \frac{1}{\nu}\left(\frac{L}{2} - \delta\right)^2 \approx \frac{1}{\nu}\frac{L^2}{4}. \tag{2-7}$$

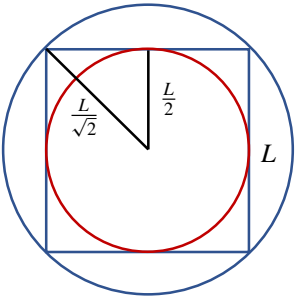

Figure 2. Upper and lower bounds of first hitting time using inscribed and circumscribed circles.

For the two-dimensional case, we will derive formally lower and upper bounds on the expected hitting time in the case $A = 0$. These bounds will serve as a calibrating tool for our numerical scheme to ensure that we are not under-resolving our computation. We are deriving analytic bounds since we are not aware of a compact analytical formula for the expected hitting time in the case of the torus. Recall that our 2-dimensional setting is an agent starting at $(0, 0)$ and performing a 2-dimensional Brownian motion $\sqrt{\nu}B_t$ until hitting a disk of radius δ located at the origin $(0, 0)$. Thus we need bounds on

$$\mathbb{E}^{(0,0)}[T_{2D}], \quad T_{2D} := \inf\left\{t \;\middle|\; \left|\sqrt{\nu}B_t - \left(\tfrac{L}{2}, \tfrac{L}{2}\right)\right| = \delta\right\},$$

where the Brownian motion is happening on $[0, L)^2$ with periodic boundary conditions. To get lower and upper bounds on this expectation, we will use two annuli centered at $\left(\frac{L}{2}, \frac{L}{2}\right)$ with inner radius δ and outer radii $\frac{L}{2}$ and $\frac{L}{\sqrt{2}}$, respectively. The boundary condition on the outer boundaries of the annuli will be reflective. Since the smaller annulus is inscribed into the torus and the larger one encompasses it (see Figure 2), we anticipate that our expected hitting time is sandwiched between the expected hitting times for the two annuli. We use the reflective boundary condition since it is a better proxy for the periodic wrap-around that happens on the torus. The connection with the PDE that we described in the previous calculation holds in the 2-dimensional setting, and the reflective Brownian motion is known to correspond to the Neumann boundary condition; see, e.g., [Bass 1998]. Thus for the smaller annuli $A_{\delta,L/2}$ case, the expected hitting time $g(x)$ of a Brownian motion starting at $x \in A_{\delta,L/2}$ satisfies

$$\tfrac{1}{2}\nu\Delta g(x_1, x_2) = -1, \quad (x_1, x_2) \in A_{\delta,L/2}, \quad r = \sqrt{\left(x_1 - \tfrac{L}{2}\right)^2 + \left(x_2 - \tfrac{L}{2}\right)^2}, \tag{2-8a}$$

$$g|_{\partial B((L/2,L/2);\delta)} = 0, \quad \partial_r g|_{\partial B((L/2,L/2);L/2)} = 0. \tag{2-8b}$$

Here $B(x; R)$ denotes the ball centered at x and with radius R. The Dirichlet boundary condition for $r = \delta$ describes the fact that the particle gets absorbed at the inner

boundary. Since the particle is assumed to be reflected at the outer boundary, the Neumann boundary condition is imposed at $r = \frac{L}{2}$. As the equation is radially symmetric, we can change to polar coordinates and solve it explicitly. The solution is given by

$$g(r) = \frac{\delta^2}{2\nu} - \frac{r^2}{2\nu} + \frac{L^2}{4\nu} \log \frac{r}{\delta}. \tag{2-9}$$

To estimate the lower bound for the expected first hitting time, we first ignore the time it takes for the particle to reach the circle $\partial B\left(\left(\frac{L}{2}, \frac{L}{2}\right); \frac{L}{2}\right)$. Once the particle reaches the circle $\partial B\left(\left(\frac{L}{2}, \frac{L}{2}\right); \frac{L}{2}\right)$, we estimate the lower bound of the expected first hitting time by picking $r = \frac{L}{2}$ in the formula above. Hence, we obtain

$$\mathbb{E}^{x_0}[T_{2D}] \geq \frac{\delta^2}{2\nu} - \frac{L^2}{8\nu} + \frac{L^2}{4\nu} \log \frac{L}{2\delta}.$$

Then we perform similar calculations as in (2-8) $\left(\text{with } \frac{L}{2} \text{ replaced by } \frac{L}{\sqrt{2}}\right)$ to obtain the heuristic upper bound

$$\mathbb{E}^{x_0}[T_{2D}] \leq \frac{\delta^2}{2\nu} - \frac{L^2}{4\nu} + \frac{L^2}{2\nu} \log \frac{L}{\sqrt{2}\delta}.$$

3. Numerical result

3.1. ***Numeric scheme.*** To simulate the solution to the stochastic differential equation

$$d\boldsymbol{X}_t = \begin{pmatrix} Au((X_2)_t) \\ 0 \end{pmatrix} + \sqrt{\nu} d\boldsymbol{B}_t, \tag{3-1}$$

we use the Euler–Maruyama method. We take

$$u(x_2) = \sin\left(\frac{2\pi\left(x_2 - \frac{L}{2}\right)}{L}\right);$$

recall that the target is located at $x_2 = \frac{L}{2}$, so the fluid flow can be thought of as taken relative to the target. For very large amplitudes of A (specifically we took 800 as threshold in the simulation), we saturate the value of the shear replacing $Au((X_2)_t)$ with $800Au((X_2)_t)/|Au((X_2)_t)|$ if $|Au((X_2)_t)| > 800$. We do this in order not to take the time step excessively small. We ran several simulations to check that this cutoff procedure has no effect on the expected hitting time. In any case, only structure (mostly, the shear rate) of u near the egg should affect the result, and the cutoff only applies some distance away from the egg. The numerical experiments confirmed this heuristic.

3.2. ***Parameters.*** Table 1 gives the list of parameters used in the simulation in the natural units (the numerical values differ for two parameters — that is discussed below).

parameters	value/range in biology	value/range in simulation
diffusion coeff.	$\sim 600\,(\mu\text{m})^2/\text{s}$	$0.25(0.1\,\text{mm})^2/(4\text{s}) = 625\,(\mu\text{m})^2/\text{s}$
egg radius	$100(\mu\text{m})$	$1(0.1\,\text{mm}) = 100\,(\mu\text{m})$
box size	$\sim 8000\,(\mu\text{m})$	$50-1000(0.1\,\text{mm}) = 5000-100000\,(\mu\text{m})$
shear rate	$0-12(\text{s}^{-1})$	$0-100\,(4\text{s})^{-1} = 0-25\,(\text{s}^{-1})$

Table 1. Parameters used in the simulation.

Here the shear rate is defined as the ratio A/L. The ranges of the parameters are largely inspired by the biological experiments [Zimmer and Riffell 2011]. The typical abalone egg size is 0.2 mm. The Taylor–Couette tank used in the experiment has a distance of about 8 mm between concentric cylinders, and the shear rates tested range between 0 and $10\,\text{s}^{-1}$. Our simulation covers these ranges of parameters and more. One parameter that is not immediate to estimate is the diffusion coefficient. In the absence of chemical stimuli, sperm move in some direction for a while, then change the direction randomly. The speed v_0 of the sperm is about 0.05 mm/s. Let t be the time that sperm maintains direction. Then over the larger time $T = nt$, the displacement D_T is given by $D_T = \sum_{i=1}^{n} X_i$, where X_i are independent 2-dimensional random variables with amplitude $v_0 t$ and random direction uniformly distributed over $[0, 2\pi)$. We can estimate the expected displacement by

$$\mathbb{E}(D_T^2) = \mathbb{E}\left(\sum_{i=1}^{n} X_i \cdot \sum_{j=1}^{n} X_j\right) = n\mathbb{E}(X_i^2) = nv_0^2t^2 = Tv_0^2t.$$

Now for a 2-dimensional Brownian motion, we have $\mathbb{E}(B_T^2) = 4\nu T$, where ν is the diffusion coefficient. Thus in two dimensions it is reasonable to adopt an estimate $\nu = \frac{1}{4}v_0^2 t$. The only parameter that we do not have readily available is t, but looking at the trajectories of sperm motion provided in [Zimmer and Riffell 2011], taking $t \sim 1$ s appears to be reasonable. This leads to the estimate $\nu \approx 0.06\,(0.1\,\text{mm})^2/\text{s} = 600\,\mu\text{m}^2/\text{s}$. In the numerical simulation, we choose not to have a very small diffusion coefficient and pick $\nu_{\text{num}} = 0.25\,(0.1\,\text{mm})^2/(4\text{s}) = 625\,(\mu\text{m})^2/\text{s}$, which is equivalent to changing time from one second to roughly 4 second effective units. The only parameter in the table that gets affected is the shear rate, that in the new units ranges between 0 and 100 in our simulation. Although the parameter ranges are coordinated with the experiment [Zimmer and Riffell 2011], we find it likely that they are relevant in a wider range of biological applications.

4. Discussion of the numerical results

In the 1-dimensional case (Figure 3, left), we calculate the expected first hitting time of the Brownian motions $\frac{\sqrt{2}}{2}\,dB_t$ on the torus $\mathbb{T}$ numerically. Our numerical

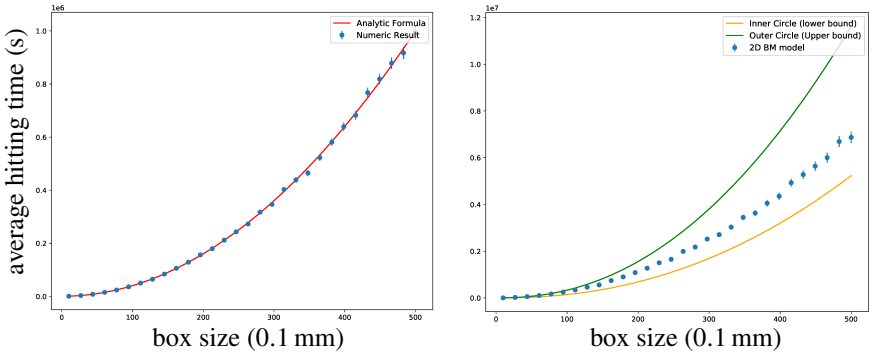

Figure 3. Comparison between the numerical result and the analytical result in 1-dimensional (left) and 2-dimensional (right) Brownian motion ($\nu = 0.25\ (0.1\,\text{mm})^2/(4\,\text{s}) = 625\ (\mu\text{m})^2/\text{s}$).

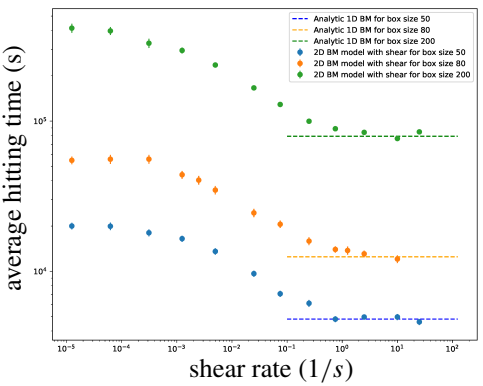

Figure 4. Convergence of the expected first hitting time of the 2-dimensional searching agent ($\nu = 0.25(0.1\,\text{mm})^2/(4\text{s}) = 625(\mu\text{m})^2/\text{s}$).

result matches the theoretical expected first hitting time in (2-7) with

$$\nu = 0.25\ (0.1\,\text{mm})^2/(4\,\text{s}) = 625\ (\mu\text{m})^2/\text{s}.$$

In the 2-dimensional case (Figure 3, right), we calculate the expected first hitting time of the Brownian motion $\sqrt{\nu} dB_t = \frac{1}{2} dB_t$ on the torus numerically. Our result is consistent with the upper and lower bounds obtained in Section 2.1.

In Figure 4, we observe that the expected first hitting time is a monotone decreasing function of the shear rate (A/L). Moreover, significant decay of about 50% happens at small shear rate of only $\sim 0.02\,\text{s}^{-1}$ (0.1 when using $1/(4\,\text{s})$ units). A similar effect was also observed in [Zimmer and Riffell 2011], where the increase in fertilization success is quite dramatic for the low values of shear — however, it peaks for the shear rate $0.1 - 0.5\,\text{s}^{-1}$ and starts to decline gradually afterwards.

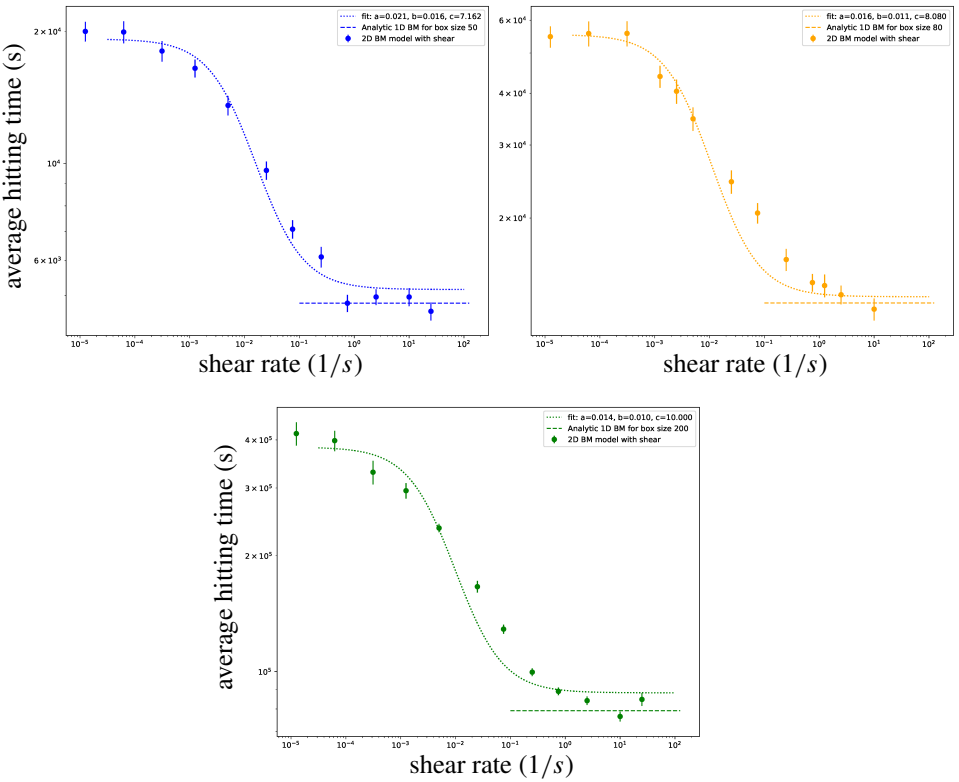

Figure 5. Curve fitting for the hitting time decay as shear increases. Box size: $50(0.1\text{ mm}) = 5000\,\mu$m (top left), $80(0.1\text{ mm}) = 8000\,\mu$m (top right), $200(0.1\text{ mm}) = 20000\,\mu$m.

We also fit the data points of the expected first hitting time with the formula

$$y = \exp\left(\frac{a}{b+x} + c\right), \quad a, b, c \in \mathbb{R}, \tag{4-1}$$

where x is the shear rate and y is the expected first hitting time. The results are presented in Figure 5. We note that these graphs differ from fertilization success rate graphs for the experiment [Zimmer and Riffell 2011] in that the expected time is decaying monotonically — there is no optimal shear rate after which the graph reverses. Indeed, the decrease of fertilization rate for large shears is likely not due to the difficulty of finding the eggs, but the sperm's inability to stay close for a necessary period of time. It is an interesting question if a combination of shear flow and chemotaxis can replicate some of this success deterioration for larger shears, or it is entirely due to more detailed mechanics of fertilization. This question will be considered elsewhere.

Acknowledgements

This research was carried out as a part of the DoMath program at Duke University. Support provided by Duke University and DoMath program is gratefully acknowledged. Y. Gong acknowledges partial support of the NSF-DMS grant 1848790. S. He acknowledges partial support of the NSF-DMS grant 2006660. A. Kiselev acknowledges partial support of the NSF-DMS grant 2006372 and of the Simons Fellowship.

References

[Bass 1998] R. F. Bass, *Diffusions and elliptic operators*, Springer, 1998. MR Zbl

[Durrett 1996] R. Durrett, *Stochastic calculus*: *a practical introduction*, CRC Press, Boca Raton, FL, 1996. MR Zbl

[Freidlin and Wentzell 2012] M. I. Freidlin and A. D. Wentzell, *Random perturbations of dynamical systems*, 3rd ed., Grundl. Math. Wissen. **260**, Springer, 2012. MR Zbl

[Iyer et al. 2010] G. Iyer, A. Novikov, L. Ryzhik, and A. Zlatoš, "Exit times of diffusions with incompressible drift", *SIAM J. Math. Anal.* **42**:6 (2010), 2484–2498. MR Zbl

[Kloeden and Pearson 1977] P. E. Kloeden and R. A. Pearson, "The numerical solution of stochastic differential equations", *J. Austral. Math. Soc. Ser. B* **20**:1 (1977), 8–12. MR Zbl

[Øksendal 1989] B. Øksendal, *Stochastic differential equations*: *an introduction with applications*, 2nd ed., Springer, 1989. MR Zbl

[Riffell and Zimmer 2007] J. A. Riffell and R. K. Zimmer, "Sex and flow: the consequences of fluid shear for sperm-egg interactions", *J. Exp. Biol.* **210**:20 (2007), 3644–3660.

[Riffell et al. 2004] J. A. Riffell, P. J. Krug, and R. K. Zimmer, "The ecological and evolutionary consequences of sperm chemoattraction", *Proc. Natl. Acad. Sci. USA* **101**:13 (2004), 4501–4506.

[Zimmer and Riffell 2011] R. K. Zimmer and J. A. Riffell, "Sperm chemotaxis, fluid shear, and the evolution of sexual reproduction", *Proc. Natl. Acad. Sci. USA* **108**:32 (2011), 13200–13205.

Received: 2021-03-05 Revised: 2021-09-09 Accepted: 2021-09-22

despoina.chouliara@duke.edu *Duke University, Durham, NC, United States*

yishu.gong@duke.edu *Department of Mathematics, Duke University, Durham, NC, United States*

simhe@math.duke.edu *Department of Mathematics, Duke University, Durham, NC, United States*

kiselev@math.duke.edu *Department of Mathematics, Duke University, Durham, NC, United States*

haechan.lim@duke.edu *Duke University, Durham, NC, United States*

omar@math.duke.edu *Department of Mathematics, Duke University, Durham, NC, United States*

kfp8@duke.edu *Duke University, Durham, NC, United States*

involve

msp.org/involve

INVOLVE YOUR STUDENTS IN RESEARCH

Involve showcases and encourages high-quality mathematical research involving students from all academic levels. The editorial board consists of mathematical scientists committed to nurturing student participation in research. Bridging the gap between the extremes of purely undergraduate research journals and mainstream research journals, *Involve* provides a venue to mathematicians wishing to encourage the creative involvement of students.

See inside back cover or msp.org/involve for submission instructions. The subscription price for 2022 is US $/year for the electronic version, and $/year (+$, if shipping outside the US) for print and electronic. Subscriptions, requests for back issues and changes of subscriber address should be sent to MSP.

Involve (ISSN 1944-4184 electronic, 1944-4176 printed) at Mathematical Sciences Publishers, 798 Evans Hall #3840, c/o University of California, Berkeley, CA 94720-3840, is published continuously online. Periodical rate postage paid at Berkeley, CA 94704, and additional mailing offices.

Involve peer review and production are managed by EditFlow® from Mathematical Sciences Publishers.

PUBLISHED BY

mathematical sciences publishers

nonprofit scientific publishing

http://msp.org/

involve
2022 vol. 15 no. 1